FERMILAB-Conf-96/149-E
D0

Electroweak Results from D0

Kathleen Streets
For the D0 Collaboration

Fermi National Accelerator Laboratory
P.O. Box 500, Batavia, Illinois 60510

June 1996

Submitted for the proceedings of the *XXXIst Rencontres de Moriond on Electroweak Interactions and Unified Theories*, Les Arcs, Savoie, France, March 16-23, 1996

Operated by Universities Research Association Inc. under Contract No. DE-AC02-76CHO3000 with the United States Department of Energy

Disclaimer

ELECTROWEAK RESULTS FROM DØ

Kathleen Streets
(for the DØ Collaboration)
New York University, New York, NY 10003, USA

Abstract

The DØ experiment collected $\approx$ 15 pb^{-1} in run 1A (1992-1993) of the Fermilab Tevatron Collider using $p\bar{p}$ collisions at $\sqrt{s} = 1.8$ TeV and $\approx$ 89 pb^{-1} in run 1B (1994-1995). Results from analyses of electroweak interactions are presented including the W and Z production cross sections and the W width measurements. From the run 1A data sample of $W \to e\nu$ and $Z \to ee$ decays, the W boson mass was measured to be 80.350 ± 0.270 GeV/c^2. Analyses which measured di-boson production are presented together with limits that were placed on the coupling parameters.

Submitted for the proceedings of the *XXXIst Rencontres de Moriond on Electroweak Interactions and Unified Theories*, Les Arcs, Savoie, France, March 16-23, 1996

1 Introduction

Results are presented from data collected by the DØ experiment that test the Standard Model (SM) of electroweak interactions[1]. Measurements are presented of the W and Z boson production cross sections, the W decay width and the W mass. Triple gauge boson couplings are studied through measurements of di-boson production and limits are set on anomalous couplings.

2 The Detector

The DØ detector was designed to study a variety of high transverse momentum (p_T) physics topics and has been described in detail elsewhere[2]. It does not have a central magnetic field, making possible a compact, hermetic detector with almost full solid angle coverage. The detector has an inner tracking system which measures charged tracks to a pseudo-rapidity $\eta < 3.2$, where $\eta = -\ln\tan\frac{\theta}{2}$ and θ is the polar angle. The tracking system is surrounded by finely-segmented uranium liquid-argon calorimeters (one central and two end-caps). Electrons and photons were identified by the shape of their energy deposition in the calorimeter and a matching track (for electrons). The energy (E) was measured by the calorimeter with a resolution of $\approx 15\%/\sqrt{E}$ (GeV). Muons were identified and their momentum measured using magnetized iron toroids that are situated between the first two of three layers of proportional drift tubes. The muon momentum resolution is $\sigma(1/p) = 0.18(p-2)/p^2 \oplus 0.008$ (p in GeV/c). Neutrinos were not identified in the detector but their transverse momentum was inferred from the missing transverse energy in the event: $\vec{\not\!\!E}_T = -\sum_i E_i \sin\theta$, where the sum i extends over all cells in the calorimeter.

The leptonic decay modes, $W \to l\nu, Z \to ll$ with $l = e, \mu$, are used to identify the gauge bosons cleanly in most of the analyses, since it is more difficult to separate the hadronic decays of Ws and Zs from the large background of QCD interactions. These decays are characterized by a high-p_T lepton and large $\not\!\!E_T$ for Ws and two high-p_T leptons for Zs. For $W \to e\nu$ decays, the resolution in $\not\!\!E_T$ was ≈ 3 GeV and was dominated by the measurement of the energy recoiling against the W. For $W \to \mu\nu$, the muon momentum resolution dominated the $\not\!\!E_T$ resolution.

3 W and Z Production and W Width

The rate of Ws and Zs observed is proportional to the production cross section times the leptonic branching fraction. For this analysis, electrons were restricted to a region $|\eta|_e < 1.2$ or $1.5 < |\eta|_e < 2.5$ and muons to a region $|\eta|_\mu < 1.0$. The $W \to e\nu$ events were selected by requiring the transverse energy of the electron $E_T^e > 25$ GeV and $\not\!\!E_T > 25$ GeV and the $Z \to ee$ events were required to have two e's with $E_T > 25$ GeV. The $W \to \mu\nu$ event selection required $p_T(\mu) > 20$ GeV and $\not\!\!E_T > 20$ GeV and the $Z \to \mu\mu$ selection required $p_T > 15, 20$ GeV for the two μ's. The number of events observed and the product $\sigma \cdot B$ from the run 1A data[3] are shown in table 1. The results are consistent with the SM predictions[3,4,5,6] of $\sigma_W \cdot B \to l\nu = 2.42^{+0.13}_{-0.11}$ (nb) and $\sigma_Z \cdot B \to ll = 0.226^{+0.011}_{-0.009}$ (nb). The predictions use CTEQ2M parton distribution functions (pdf). Also shown in the table are statistics from the preliminary run 1B analysis.

The ratio of the W and Z production cross sections can be used to measure the leptonic branching ratio $B(W \to l\nu)$ and the W width (Γ_W). From the measured width a limit may be placed on unexpected decay modes of the W. Many common systematic errors, including the luminosity error, cancel in the ratio:

$$R = \frac{\sigma_W \cdot B(W \to l\nu)}{\sigma_Z \cdot B(Z \to ll)} = \frac{\sigma_W}{\sigma_Z} \frac{\Gamma(W \to l\nu)}{\Gamma(Z \to ll)} \frac{\Gamma_Z}{\Gamma_W}$$

Using the run 1A results above for $\sigma \cdot B$ and combining the electron and muon measurements, we obtain $R = 10.90 \pm 0.49$. The leptonic branching fraction of the W may then be calculated, $B(W \to l\nu) = B(Z \to ll)(\sigma_Z/\sigma_W)R = (11.02 \pm 0.5)\%$ using the measured value of R, $B(Z \to ll) = (3.367 \pm 0.006)\%$ from LEP[5] and the $\sigma_W/\sigma_Z = 3.33 \pm 0.03$ from the SM prediction[3,4]. The total width of the W is then obtained from this measurement of $B(W \to l\nu)$ and the SM value[3,6] for $\Gamma(W \to l\nu) = 225.2 \pm 1.5$ MeV. The result $\Gamma_W = 2.044 \pm 0.093$ GeV, is in good agreement with the SM prediction[3,6] of 2.077 ± 0.014 GeV, and when combined with previous measurements[3,7] gives a new weighted average of $\Gamma_W = 2.062 \pm 0.059$ GeV. By comparing this value to the SM prediction, a 95% confidence level upper limit of $\Delta\Gamma_W < 109$ MeV is placed on unexpected (non-SM) decays of the W.

	$W \to e\nu$	$Z \to ee$	$W \to \mu\nu$	$Z \to \mu\mu$
# events (1A)	10388	775	1665	77
$\sigma \cdot B$ (nb)	2.36 ± 0.15	0.218 ± 0.016	2.09 ± 0.25	0.178 ± 0.032
$\approx$ # events (run 1B)	60000	5700	7700	500
luminosity analysed (1B)	76.5 pb^{-1}	89.0 pb^{-1}	55 pb^{-1}	55 pb^{-1}

Table 1: Statistics and production cross section times branching ratio for W and Z bosons.

4 W Mass

The gauge sector of the SM of electroweak interactions contains three fundamental parameters. These may be taken to be α, G_F and $\sin^2\theta_W$, all measured to $< 0.01\%$. They precisely define the W mass (M_W) at the tree level. Higher order diagrams introduce a dependence on the top quark mass and the Higgs mass. Measurements of the W and top quark masses then serve to test the SM and constrain the Higgs mass. Previous experiments[8] have measured M_W with an uncertainty of $\approx 0.2\%$.

In the analysis presented here, a sample of $W \to e\nu$ events from run 1A were used to make a new high precision measurement of the W mass. The calorimeter is not calibrated independently to the precision needed and therefore the ratio of the W to Z masses was measured and then scaled to the precisely known ($< 0.01\%$) LEP/SLC Z mass. Many systematic errors cancel in the ratio.

Experimentally, the remnants of the interaction $p\bar{p} \to W(\to e\nu) + X$, where X is due to the recoil of the W plus the underlying event, were detected. The energy of the electron (we use $E \equiv p$) and the $\vec{\not{E}}_T$, which is identified with the neutrino transverse momentum $\vec{p}_T(\nu)$, were measured. Because the longitudinal momentum of the ν is not measured, the W invariant mass cannot be constructed. Instead the distribution in transverse mass: $M_T(W) =$

$\sqrt{2p_T(e)p_T(\nu) - 2\vec{p}_T(e)\cdot\vec{p}_T(\nu)}$ is used to obtain the W mass. For Z decays, the energies of both electrons are measured and the invariant mass is reconstructed.

The $W \to e\nu$ events were selected by requiring an isolated electron with $E_T^e > 25$ GeV, W transverse momentum $p_T(W) < 30$ GeV/c and $\not{E}_T > 25$ GeV. The $Z \to ee$ events were selected by requiring two isolated electrons with $E_T^e > 25$ GeV. Electrons were required to be in the region $|\eta| < 1.2$. In this analysis, the electron angle was determined from the shower centroid of the energy cluster in the EM calorimeter and the center-of-gravity of the corresponding track. The uncertainty in determining this angle results in an uncertainty of 50 MeV/c^2 in M_W.

The mass of the W was determined by a maximum likelihood fit of the measured $M_T(W)$ distribution to Monte Carlo (MC) distributions which were generated for 21 values of M_W from 79.4 to 81.4 GeV/c^2. This fast MC simulation used a theoretical prediction of W production and decay and a parameterized model for the detector response. Z events were treated in an analagous fashion. Below is a discussion of the determination of the parameters in the MC.

The W production is modelled by the double differential cross section in $p_T(W)$ and rapidity calculated at next-to-leading order by Ladinsky and Yuan[9)] and using the MRSA[10)] pdf. Accounting for correlations, the uncertainty in the modelling of the $p_T(W)$ spectrum and in the pdf leads to an uncertainty of 65 MeV/c^2 in M_W. The W resonance is generated by a relativistic Breit-Wigner, skewed by the mass dependence of the parton luminosity. The W width is set to 2.12 ± 0.11 GeV and its uncertainty results in an uncertainty of 20 MeV/c^2 in the measured value of M_W. The decay products are generated in the W rest frame, with an angular distribution that respects the production polarization of the W, then boosted to the laboratory system. Radiative decays ($W \to e\nu\gamma$) are generated according to Berends and Kleiss[11)].

The EM calorimeter energy scale was set using $J/\psi \to ee$, $\pi^0 \to \gamma\gamma$, and $Z \to ee$ events. From test beam studies, it was determined that a linear relationship between the true and measured energies could be assumed: $E_{\rm meas} = \alpha E_{\rm true} + \delta$. Making the requirement that the peak of the Z mass be at the LEP/SLC value[12)] fixes the scale α. The value of δ is constrained by the J/ψ and π^0 data. Allowing a quadratic term in the energy response, to account for nonlinear responses at low energies, leads to the systematic error on δ. The allowed values determined for α and δ are $\alpha = 0.9514 \pm 0.0018(stat.)^{+.0061}_{-.0017}(syst.)$ and $\delta = -0.158 \pm 0.015(stat.)\ ^{+.030}_{-.210}(syst.)$ GeV. We note that if $\delta = 0$, the ratio M_W/M_Z is independent of the scale α, since it enters only through terms involving δ. The error in the EM energy scale introduces an uncertainty in the M_W of 160 MeV/c^2 and is dominated by the statistical error in determining the Z mass.

The EM energy resolution was parameterized as $\sigma/E = \sqrt{C^2 + (S/\sqrt{E_T})^2 + (N/E)^2}$ for the central calorimeter. Test beam data were used to set the sampling term, $S = 0.13$ (GeV$^{1/2}$), and the noise term, $N = 0.4$ GeV. By constraining the width of the Z invariant mass distribution in the MC to that from the data, the constant term was set to $C = (1.5\ ^{+0.6}_{-1.5})$. The uncertainty in the energy resolution leads to an uncertainty of 70 MeV/c^2 in M_W.

The recoil against the W was modelled assuming it's a single jet. The hadronic energy scale relative to the EM scale was measured using Z events by projecting the vector sum of recoil transverse momentum, $\vec{p}_T(rec)$, and the p_T of the Z measured by the two electrons, $\vec{p}_T(ee)$, along the bisector of the electron directions, defined as the $\hat{\eta}$ axis. To ensure an equivalent event topology, Z events in which one electron is in the forward region were included in this study. Fitting the distribution of the p_T-balance ($\equiv [\vec{p}_T(ee) + \vec{p}_T(rec)] \cdot \hat{\eta}$) versus $\vec{p}_T(ee)$ to

Error	$\sigma(M_W)$ MeV/c^2
Statistical	140
EM energy scale	160
Systematic (shown in detail below)	165
EM energy resolution	70
hadronic energy scale	50
hadronic energy resolution	65
# minimum bias events	60
input $p_T(W)$ distribution & pdf	65
electron angle determination	50
W-width	20
underlying event	35
non-uniform response	10
backgrounds	35
trigger & $u_{\|\|}$ efficiencies	30
radiative decays	20
fit error	5
TOTAL	270

Table 2: The statistical, scale and systematic errors on the measurement of M_W determined from a fit to the $M_T(W)$ spectrum are given.

a straight line, gave $\vec{p}_T(rec) = (0.83 \pm 0.04)\vec{p}_T(ee)$. The ± 0.04 uncertainty in the recoil scale leads to an uncertainty of 50 MeV/c^2 in M_W.

The recoil energy was smeared using the jet energy resolution determined from the test beam with a sampling term of $S = 0.80 \pm 0.20$ (GeV$^{1/2}$). The underlying event was modelled by superimposing the W event onto a minimum bias event obtained from the data. The minimum bias events were selected from a library in the same distribution of luminosity as the W event sample. The resolution in the W recoil measurement is dominated by the underlying event. The width of the p_T-balance distribution constrained the number of minimum bias events needed to simulate the W underlying event to be 0.98 ± 0.06. This uncertainty leads to an error on M_W of 60 MeV/c^2.

Biases in the event sample due to detector and reconstruction effects were modelled in the MC simulation. The trigger efficiency was measured as a function of $p_T(e)$ and $\not{E}_T$ and its uncertainty leads to an error on M_W of 20 MeV/c^2. Radiative decays caused electron mis-identification due to shower shape and isolation requirements, depending on the γ and e separation. The uncertainty on the measured M_W due to radiative decays is 20 MeV/c^2. The recoil of the W also affected the electron identification due to the recoil energy overlapping the electron energy cluster. A measure of the bias is given by the variable $u_{||} = \vec{p}_T(rec) \cdot \hat{e}$ which is defined as the projection of the p_T of the recoil in the electron direction. The efficiency of event selection as a function of $u_{||}$ was determined from the W events using the shape of the electron isolation distribution and verified using Z events in which one electron was free of any biases. The uncertainty in this $u_{||}$ efficiency gives an uncertainty in the M_W of 30 MeV/c^2.

Backgrounds to the W event sample were included in the fitting procedure by including the shape and fraction of background events. The largest source of background in the W sample is QCD multi-jet production. This background contributes $1.6 \pm 0.8\%$ to the W sample and shifts the M_W by $+33$ MeV/c^2. The other background considered was $Z \to ee$ events where one electron is not identified. This background contributes $0.43 \pm 0.05\%$ to the W sample and its effect on M_W is negligible. The uncertainty in size and shape of the backgrounds gave an uncertainty in M_W of 35 MeV/c^2. Events in which $W \to \tau\nu \to e\nu\bar{\nu}\nu$ are indistinguishable from $W \to e\nu$ decays and were therefore modelled in the simulation.

The $M_T(W)$ distribution is shown in Fig. 1a together with the distribution from the best fit value of M_W from the Monte Carlo simulation. There were 5982 events included in the fit of the data over a region 60 to 90 GeV/c^2 and the result for the W mass is $M_W = 80.350 \pm 0.140(stat.) \pm 0.160(scale) \pm 0.165(syst.)$ GeV/c^2 which gives a total error of ± 270 MeV/c^2. The errors on the W mass are given in table 2. Another measure of how accurately the MC describes the data is shown in Fig. 1b which shows the mean $u_{||}$ as a function of $p_T(W)$. Excellent agreement between the data and MC simulation is seen. Combining the new DØ result with previous measurements[8)] and taking into account the correlated errors gives a new world average of $M_W = 80.33 \pm 0.15$ GeV/c^2.

As consistency checks, the $p_T(e)$ and $p_T(\nu)$ spectra were also fit to determine M_W as shown in Fig. 1c and 1d. The fit to the $p_T(e)$ spectrum gave $M_W = 80.300 \pm 0.190(stat.)$ GeV/c^2 and the $p_T(\nu)$ fit gave $M_W = 80.045 \pm 0.260(stat.)$ GeV/c^2 with 5520 and 5457 events in the fitting region from 30 to 45 GeV/c respectively. It should be noted that the systematic error on the fit to the $p_T(\nu)$ spectrum is large compared to that from the $M_T(W)$ spectrum.

5 Anomalous Couplings

Gauge boson self-interactions are predicted due to the non-Abelian nature of the SM. The tri-linear couplings can be tested through study of di-boson production. The direct and precise measurement of the couplings are of interest since deviation from SM predictions (i.e. anomalous couplings) is a signature for new physics.

5.1 $WW\gamma$ and WWZ Couplings

The $WW\gamma$ and WWZ couplings can be measured through directly produced $W\gamma$, WW and WZ events. The SM prediction[13)] involves the variable g_1^V and $\Delta\kappa_V$ and λ_V $(V = \gamma, Z)$ which are CP-conserving coupling parameters. At the tree level, the SM predicts $\Delta\kappa = \lambda = 0$. Non-SM coupling parameters result in an increase of the production cross section and a change in the kinematic distributions. To avoid unitarity violations due to non-zero couplings, $\Delta\kappa$ and λ are parameterized as form factors with scale Λ: $\Delta\kappa \to \Delta\kappa/(1 + \frac{s}{\Lambda^2})^n$ $(n = 2)$.

DØ has directly measured[14)] the $WW\gamma$ coupling through the study of $W\gamma$ production using $p\bar{p} \to l\nu\gamma + X$ events where $(l = e, \mu)$. $W\gamma$ events were selected by requiring a lepton with $p_T > 25(15)$ GeV/C and $\not{E}_T > 25(15)$ GeV for the $e(\mu)$, respectively, and an isolated γ with $p_T > 10$ GeV/c. A total of 23 events in both channels were observed in the run 1A data sample, with an expected background of 6.4 ± 1.4 events. In an analysis of the partial 1B data sample (55.2 pb^{-1}) in the e channel, 36 events were observed with a background of 8.4 ± 1.7 events. Figure 2a shows the p_T spectrum for the data with the SM prediction and background. Limits on the coupling parameters were obtained by performing a maximum likelihood fit of the measured E_T spectrum of the γ to the sum of the prediction plus background. Preliminary results for the run 1A and 1B combined data, using a form factor $\Lambda = 1.5$ TeV, results in the 95% confidence level (CL) limits of $-1.42 < \Delta\kappa < 1.39$ $(\lambda = 0)$ and $-0.41 < \lambda < 0.40$ $(\Delta\kappa = 0)$ from $W\gamma$ production.

WW production, with both Ws decaying to leptons ($ee, e\mu, \mu\mu$) was measured[15]. One event was observed with an expected background of 0.56 ± 0.13 events in the run 1A data sample. Using a form factor scale of $\Lambda = 900$ GeV, limits of $-2.6 < \Delta\kappa < 2.8$ ($\lambda = 0$) and $-2.1 < \lambda < 2.1$ ($\Delta\kappa = 0$) were set on the coupling parameters.

The production of WW and WZ was studied by selecting events with $W \to e\nu$ and two jets[16]. From a preliminary analysis of the run 1A data, 84 ± 9.2 events were observed with an expected background of 12.2 ± 2.3 events due to QCD fakes and 62.2 ± 8.2 events due to $W+ \geq 2$ jet events. A fit to the measured $p_T(W)$ spectrum (from $W \to e\nu$) compared to predictions with non-SM couplings was performed. Using a value of $\Lambda = 1.5$ TeV, the coupling parameters were found to be $-0.9 < \Delta\kappa < 1.1$ ($\lambda = 0$) and $-0.6 < \lambda < 0.7$ ($\Delta\kappa = 0$) at a 95% CL.

The results from the $W\gamma, WW$, and WZ production analyses from the run 1A data samples were combined to obtain limits on the $WW\gamma$ and WWZ anomalous couplings. The preliminary results, which used $\Lambda = 1.5$ TeV, set 95% CL limits at $-0.71 < \Delta\kappa < 0.89$ ($\lambda = 0$) and $-0.44 < \lambda < 0.44$ ($\Delta\kappa = 0$) as shown in Fig. 2b. By combining the results from different analyses, tighter limits were placed on the parameters than when using increased statistics from one channel (as seen in the combined 1A and 1B $W\gamma$ production results).

5.2 $ZZ\gamma$ and $Z\gamma\gamma$ Couplings

The $ZZ\gamma$ and $Z\gamma\gamma$ couplings are not allowed in the SM, since the Z and γ do not couple to each other. Limits are set on their existence by measuring the direct production of $Z\gamma$ events. The couplings are described using the CP-conserving parameters h_3^V, h_4^V with $V = Z, \gamma$. The couplings are regulated by a form factor with scale Λ to preserve the unitarity bound.

The production of $Z\gamma \to ee, \mu\mu$ was measured[17], by selecting events with two high-p_T leptons and a high-p_T photon. In the run 1A data sample, six events were found in both channels with an expected background of 0.48 ± 0.06 events. This is consistent with the SM prediction of 5.1 ± 0.5 events. The observed E_T spectrum of the γ was fit to MC predictions (with $\Lambda = 500$ GeV) plus background to set limits on the coupling parameters. The 95% CL limits were set at $-1.8 < h_3^Z < 1.8$ and $-0.5 < h_4^Z < 0.5$.

From preliminary results of a partial sample (48 pb^{-1}) of the run 1B data, 16 events were observed in the $Z\gamma \to ee\gamma$ channel with an expected background of 1.2 events. This is consistent with the SM prediction of 11.5 events.

6 Conclusions

DØ has collected $\approx 100\ \text{pb}^{-1}$ of data in runs 1A and 1B of the Fermilab Tevatron Collider. Results of electroweak studies are presented from a partial data sample. The W and Z production cross sections were measured and the W width was measured to be $,_W = 2.044 \pm 0.093$ GeV. From a sample of $W \to e\nu$ and $Z \to ee$ decays, the mass of the W boson was measured to be $M_W = 80.350 \pm 0.270\ \text{GeV/c}^2$. Di-boson production was observed and limits were placed on the coupling parameters. No deviations from the Standard Model were observed. The analysis of the full data sample is in progress.

References

[1] S. Weinberg, Phys. Rev. Lett. **19**, 1264 (1967); S.L. Glashow, Nucl. Phys. **22**, 579 (1968); A. Salam, in *Elementary Particle Theory*, ed. by N. Svartholm (Almquist and Wiksell, Sweden, 1968), p. 367; S.L. Glashow, J. Illiopoulos and L. Maiani, Phys. Rev. D **2**, 1285 (1970); M. Kobayashi and M. Maskawa, Prog. Theor. Phys. **49**, 652 (1973).

[2] S. Abachi *et al.* (DØ Collaboration), Nucl. Instrum. and Methods Phys. Res., Sect. A **338**, 185 (1994).

[3] S. Abachi *et al.* (DØ Collaboration), Phys. Rev. Lett. **75**, 1456 (1995) and references therein.

[4] R. Hamberg, W.L. van Neerven, and T. Matsuura, Nucl Phys. **B359**, 343 (1991).

[5] Particle Data Group, L. Montanet *et al.*, Phys. Rev. D **50**, 1173 (1994).

[6] J.L. Rosner, M.P. Worah, and T. Takeuchi, Phys. Rev. D **49**, 1363 (1994).

[7] C. Albajar *et al.*, Phys. Lett. B **253**, 503 (1991), J. Alitti *et al.*, Phys. Lett. B **276**, 365 (1992) and F. Abe *et al.*, Phys. Rev. Lett. **73**, 220 (1994).

[8] Recent measurements are J. Alitti *et al.* (UA2 Collaboration), Phys. Lett. **B276**, 354 (1992); F. Abe *et al.* (CDF Collaboration), Phys. Rev. Lett. **65**, 2243 (1990) F. Abe *et al.* (CDF Collaboration), Phys. Rev. Lett. **75**, 11 (1995) F. Abe *et al.* (CDF Collaboration), Phys. Rev. **D52**, 4784 (1995).

[9] G. Ladinsky and C.P. Yuan, Phys. Rev. D **50**, 4239 (1994).

[10] A.D. Martin, R.G. Roberts, W.J. Stirling, Phys. Rev. D **50** 6734 (1994) and Phys. Rev. D **51** 4756 (1995).

[11] F.A. Berends and R. Kleiss, Z. Phys. **C27** 265 (1985).

[12] P. Renton, "Precision Tests of Electroweak Theories," Lepton-Photon Conference, Beijing, P.R. China (1995), OUNP-95-20.

[13] K. Hagiwara, R.D. Peccei, D. Zeppenfeld, and K. Hikasa, Nucl. Phys. **B282**, 253 (1987).

[14] S. Abachi *et al.* (DØ Collaboration), Phys. Rev. Lett. **75**, 1034 (1995).

[15] S. Abachi *et al.* (DØ Collaboration), Phys. Rev. Lett. **75**, 1023 (1995).

[16] S. Abachi *et al.* (DØ Collaboration), submitted to Phys. Rev. Lett.

[17] S. Abachi *et al.* (DØ Collaboration), Phys. Rev. Lett. **75**, 1028 (1995).

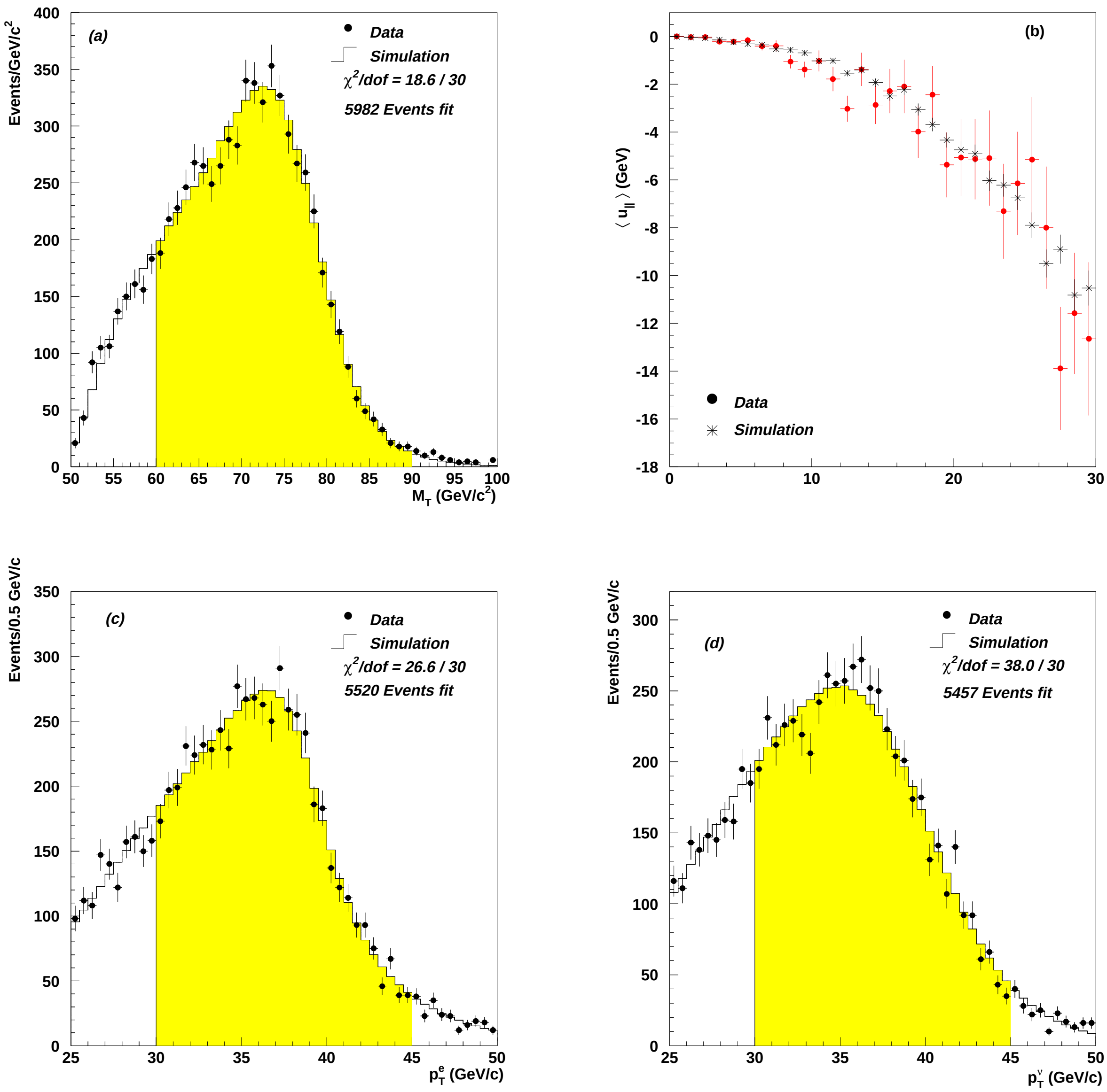

Figure 1: (a) The $M_T(W)$ distribution from data and the MC simulation at the best fit value of M_W. The fit had a $\chi^2/dof = 18.6/30$ from 5982 events over the region $60-90$ GeV (shown in shaded region of histogram). (b) Comparison of the mean $u_{||}$ versus $p_T(W)$ from data and the MC simulation. (c) The comparison of the $p_T(e)$ distribution from the data and MC simulation at the best fit value of M_W. The fit had a $\chi^2/dof = 26.6/30$. (d) The comparison of the $p_T(\nu)$ distribution from the data and MC simulation at the best fit value of M_W. The fit had a $\chi^2/dof = 38.0/30$.

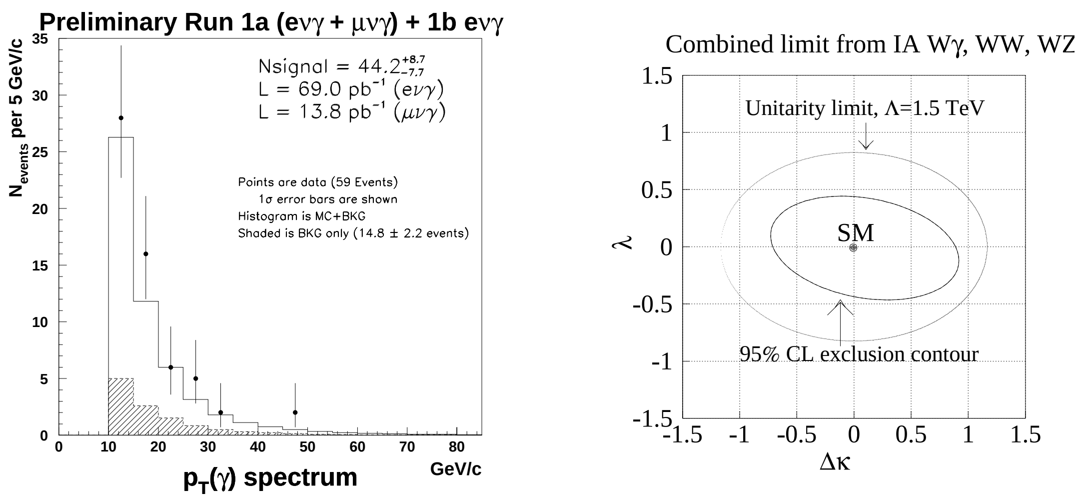

Figure 2: (a) The $p_T(\gamma)$ spectrum from $W\gamma$ events compared to the MC plus background prediction (open histogram) and to the background (shaded histogram). (b) Contour plot in λ versus $\Delta\kappa$ showing the limits obtained from the combined run 1A results from $W\gamma$, WW, and WZ production. The inner contour is the 95% CL limit and the outer contour is the unitarity limit.